Proceedings of the First European Conference on Space Debris, Darmstadt, Germany, 5-7 April 1993 (ESA SD-01)

MODEL FOR PREDICTING MICROMETEOROID/DEBRIS IMPACTS AND DAMAGE TO COMPOSITE MATERIALS

R. C. Tennyson and G. Manuelpillai
University of Toronto Institute for Aerospace Studies, Toronto, Ontario, Canada

D. G. Zimcik
Space Mechanics, Canadian Space Agency, Ottawa, Ontario, Canada

ABSTRACT

This report first presents an analysis of the published micrometeoroid/debris impact data observed on the Long Duration Exposure Facility (LDEF) which was in orbit for about 5.75 years. LDEF impact data were obtained as a function of angular location relative to the ram direction. Thus it was possible to develop a nomogram that can be used to estimate the total number of impacts that could be expected on a space structure as a function of time in orbit, angular location relative to ram and exposed surface area based on simple extrapolation/interpolation of the LDEF data. Application of the nomogram is then made to illustrate the total cumulative damage that could be expected over a 30-year lifetime in space for an exposed structure. Impact damage data on LDEF composites are presented together with ground-based hypervelocity test results. It is intended to correlate particle size with damage area for composite laminates.

1. ANALYSIS OF LDEF MICROMETEOROID/DEBRIS IMPACT DATA

From the individual LDEF experiment trays, tables of micrometeoroid/debris impact feature sizes were compiled in Ref. 1. This data was then summarized for each longitudinal panel to yield an angular (θ) distribution of total impacts around LDEF after 5.75 years in low Earth orbit. Figure 1 presents two distributions based on the "total" reported hits that were recorded by unaided visual observation, and those hits which were ≥0.5 mm in size. It should be noted that the data shown are strictly valid only at θ = 0°, ±30°, ±60°, 90°, ±120°, ±150°, 180°, and the curves cannot be integrated to give a total number of impacts. This curve has not been corrected for the 8° yaw angle of LDEF.

Based on the number distribution presented in Fig. 1, it is possible to construct a general purpose nomogram which permits a user to estimate the total number of impacts on a satellite or component (at the LDEF nominal altitude and inclination) for any value of time in orbit, angular location around the satellite or space structure (constrained by $\theta_n = n \times 30°$ where n = 0, 1, 2, ... 12, corresponding to a 12-sided polygon model of the satellite or component), and exposed area. For example, Figure 2 presents the nomogram for LDEF based on a longitudinal panel area of ~10 m^2, assuming a nominal impact fluence of 300 impacts/m^2. The example panel shown in Fig. 2 corresponds to θ = 30°. Thus the intersection of θ = 30° and the LDEF time in orbit axis (~5.75 years) yields an impact fluence of ~300 impacts/m^2. Following up along this constant fluence curve until one intersects the desired panel area (10 m^2), one can then translate horizontally across the graph to the "Number of Impacts" ordinate. For this example, one obtains N ≅ 3100 which agrees with the number plotted in Fig. 1.

Using the LDEF data from Fig. 1, knowing panel areas and total time in orbit, one can construct a general purpose nomogram for varying areas of exposure and impact fluence levels as shown in Fig. 3. Once again it must be stressed that these curves can only be used to estimate the total number of impacts at discrete angles defined by $\theta_n = n \times 30°$, n = 0, 1, ..., 12, and are strictly valid for an LDEF average altitude of ~463 km and inclination of 28.5°. It is shown in Ref. 2 how to correct these numbers for different altitudes and orbital inclinations. The population growth in debris can also be incorporated.

As an example on how to use the nomogram and the 12-sided polygon model to calculate the number of impacts on a structure, consider the case of a circular cylinder, 0.5 m in diameter, 10 m long, after 30 years in low Earth orbit. The following results were obtained on the total number of hits on each panel (Nn) for n = 1, 2, ..., 12 together with the average impact separation distance (Dn), assuming a uniform distribution.

(i) Panel Area (A)

$c = 2R \sin \phi$

For the 12-sided polygon $\phi = 15°$

$\therefore c = 0.13$ m and $A \equiv 1.3$ m^2

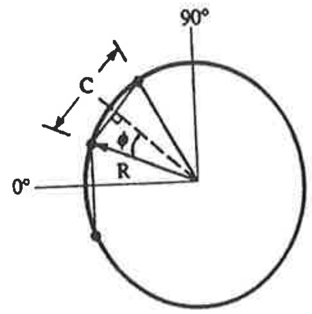

(ii) N_n Distribution from Fig. 3 (30 years)

θ_n^o	N_n (est.)	D_n (cms)
0	2070	2.5
30	2070	2.5
60	1680	2.8
90	1100	3.4
120	450	5.4
150	325	6.3
180	290	6.7

θ_n^o	N_n (est.)	D_n (cms)
-30	2260	2.4
-60	1680	2.8
-90	615	4.6
-120	550	4.9
-150	225	7.6

Although the particle flux LDEF was not strictly uniform in time, averaging over long periods of time (of the order of many months) is a reasonable approximation.

2. MICROMETEOROID/DEBRIS IMPACTS ON EXPERIMENT AO180

Experiment AO180 (Ref. 3) consisted of various graphite, aramid and boron fiber-reinforced epoxy materials mounted at station D-12, about 82° from the LDEF velocity vector. The exposed surface area was ~0.6 m^2 and was subjected to a total of 84 hits. The predicted number of impacts for this area after 5.75 years is ~80, based on the nomogram in Fig. 3 (assuming $\theta = 90°$). This agreement is particularly noteworthy since it demonstrates that after sufficient exposure time in orbit, one can predict the number of impacts likely to occur in relatively small areas.

From a detailed inspection of the composite samples (both tubes and flat plates), only 10 of the 84 hits were found on these materials, the balance located on end fixtures and the aluminum base-plates used to mount the specimens.

Micrometeoroid/debris impacts on polymer matrix composites do not produce the typical hemispherical craters found on metallic structures. Rather, because of the brittle nature of the resin matrix, one generally finds penetration holes with adjacent surface damage, some internal ply delamination and local fiber fractures. For brittle fibers such as graphite, the impact and exit holes exhibit brittle fiber fractures as shown in Fig. 4, as well as rear surface spallation [5208/T300; $(\pm45°)_S$]. Note that the spallation damage-to-hole size ratio is about 5:1. On the other hand, tough non-brittle fibers such as aramid fail in a "brush or broom" mode surrounding the impact damage region. Figure 5 presents impacts on a single Kevlar®/epoxy tube [SP-328, $(\pm45)_{4S}$]. It can be seen that two penetrations occurred with one grazing (or low energy) impact that produced only local surface damage. From the enlargements, it was possible to scan the images to calculate the surface damage area and impact hole size. These images were digitized using a Houston Instruments "Hipad" digitizer to obtain an accurate reproduction of the impact site (~200 data points on average). The X-Y coordinates of the digitized photograph were then analysed using spreadsheet/graphics programs. A trapezoidal model was used to numerically integrate the digitized image to obtain damage area and crater size (assuming a circular hole).

A summary of these results is given in Table 1. Such data will be useful for estimating total damage on composite structures that arises from micrometeoroids/debris. Note that the penetration depth was based on the image enhanced backlighting technique, which is useful for translucent materials.

Using only the Kevlar®/epoxy impact data, one can construct a plot of surface damage area vs. major axis length, as shown in Fig. 6. It would appear that an elliptical model can be used to describe the damage area for oblique impacts.

Figure 7 presents an overview of four cross-sections of different polymer matrix composites located at four different angular positions around LDEF. One can readily see the change in profile features as one goes from the 'ram' direction (0°) to the 90° position. There is no doubt that atomic oxygen plays a major role in the development of these features, but the larger surface pits may well be due to microparticle impacts.

3. HYPERVELOCITY IMPACT SIMULATIONS

Hypervelocity particle impact tests have been carried out at the Space Power Institute of Auburn University. Experiments were performed with aluminum oxide particles ≤ 100 μ diameter impacting over a velocity range of 5~11 km/s. At this point in time, only PEEK/graphite laminates have been studied in terms of the resulting impact craters and damage areas. Figure 8 shows a typical 'normal' impact feature where one can see associated microcracking in adjacent plies. Based on these results, a graph of damage area vs. 'equivalent' crater diameter* was constructed for the normal impact case, as shown in Fig. 9. The intent here is to develop a correlation between particle size, crater diameter and damage area for different composite material systems using ground-based facilities. Once such correlations are obtained, one can then estimate particle size distributions based on LDEF damage area measurements from various composite samples. Since the micrometeoroid/debris environment is characterized in terms of particle size vs. flux distribution, it should be possible to estimate total damage to a material surface using these correlations and the nomogram in Fig. 3. Corrections for altitude and inclination variations can be taken into account.

ACKNOWLEDGEMENT

This research was sponsored by the Space Mechanics Directorate of the Canadian Space Agency under Contract No. 9F009-1-1435/01-SR. The authors wish to express their great appreciation to the other LDEF experimenters who provided composite samples from different locations on LDEF. Finally, we wish to thank Dr. Frank Rose of the Space Power Institute at Auburn University for providing the hypervelocity impact tests.

* using a circle having an equivalent damage area.

REFERENCES

1. "Micrometeoroid and Orbital Debris Impact Features Documented on the Long Duration Exposure Facility — A Preliminary Report," LDEF SIG, NASA JSC, 1990.
2. "Analysis of LDEF Micrometeoroid/Debris Data and Damage to Composite Materials," Proc. NASA Second LDEF Post-Retrieval Symposium, June 1992.
3. "Composite Materials in Space — Results from the LDEF Satellite," R. C. Tennyson, J. Canadian Aeronautics and Space Institute, Vol. 37, No. 3, Sept. 1991.

Material Type	Sample Type	Number of Plies	Sample No.	Surface Damage Area (mm^2)	Hole Area (mm^2)	Nominal Hole Diameter (mm)	Particle Penetration Depth (Number of plies)
Graphite/Epoxy (T300/5208)	Plate	4		0.222	0.222		>4
Graphite/Epoxy (SP 288/T300)	Tube	4	1T10	1.064	0.083	0.325	>4
Aramid* Fiber/Epoxy (SP 328)	Tube	4	2T2	1.162	0.036	0.215	1~2
"	Tube	4	2T4	0.498	0.015	0.139	~1
"	Tube	4	2T11	0.423	0.018	0.152	~1
"	Tube	4	2T16	1.253	0.076	0.312	2~3
"	Tube	4	2T17(1)	0.223	—	—	1~2
			2T17(2)	1.445	0.033	0.204	2~3
			2T17(3)	0.370	—	—	~1
			2T17(4)	0.881	0.020	0.159	2~3

*Kevlar

Table 1. Summary of Impact Features on Composite Specimens (Experiment AO180)

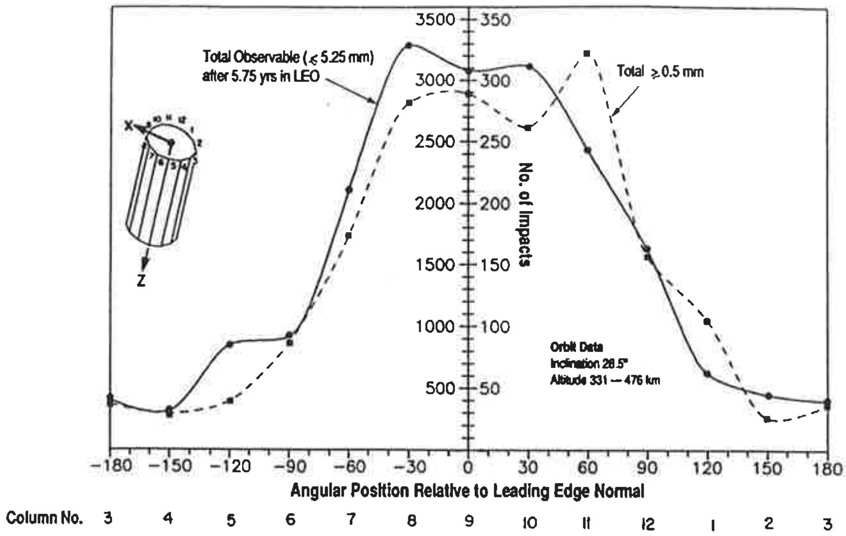

Figure 1. Circumferential distribution of micrometeoroid/debris impacts on LDEF (NASA M&D/SIG Report; Aug. 1990)

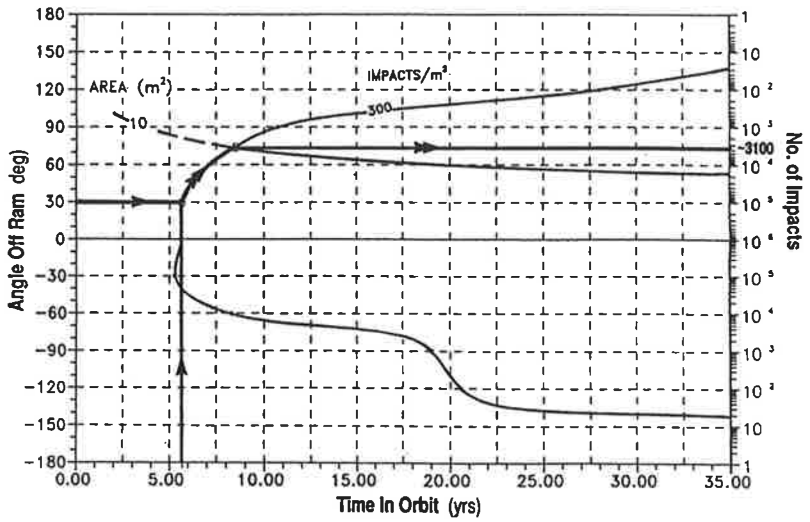

Figure 2. Nomogram for LDEF

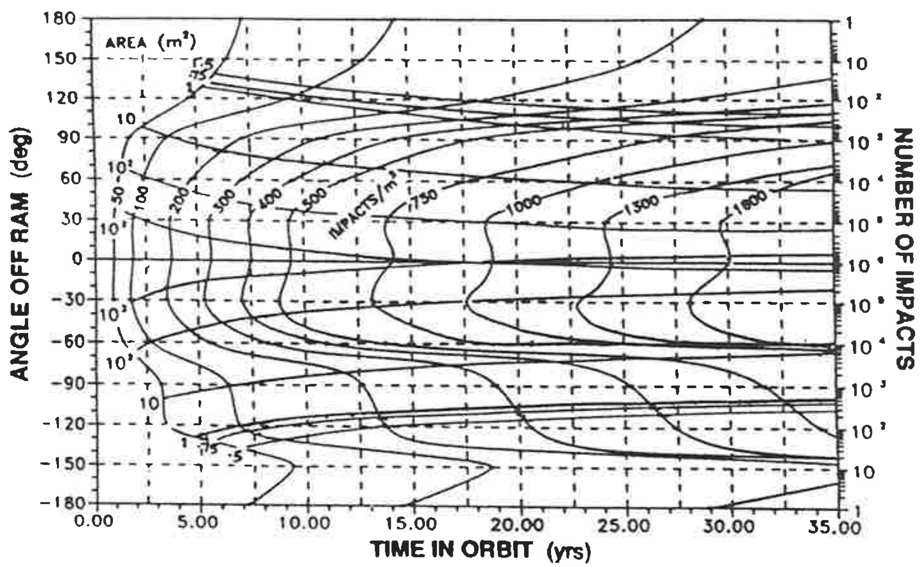

Fig. 3 Nomogram for estimating total number of micrometeoroid/debris impacts for arbitrary exposed surface areas as a function of angle off ram and time in orbit

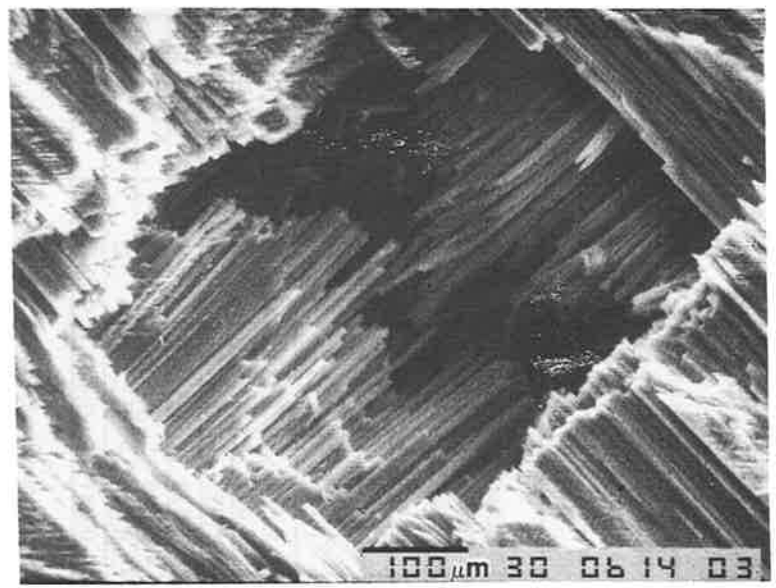

View of front face impact hole (x100)

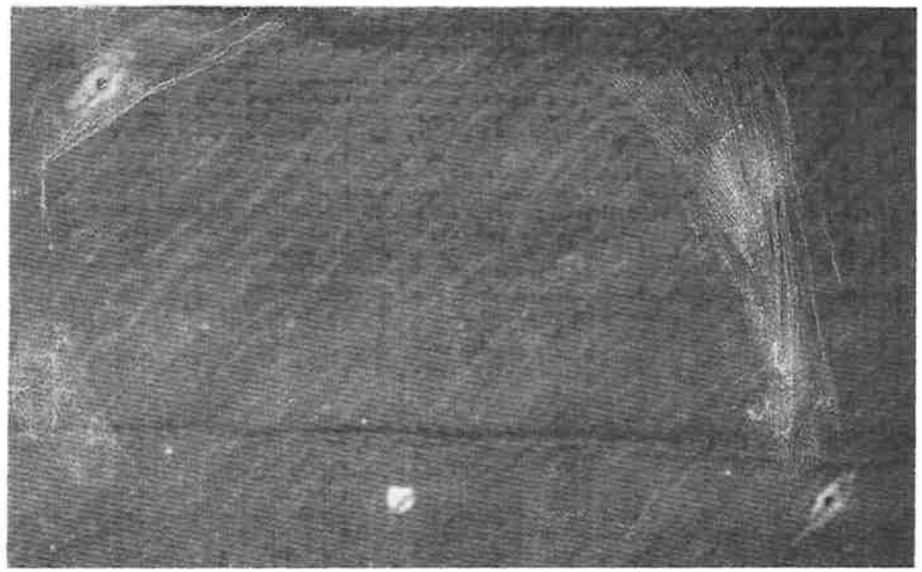

Fig. 5 Micrometeoroid/Debris Impacts on Kevlar®/Epoxy Tube [SP-328, $(\pm 45°)_{4S}$]

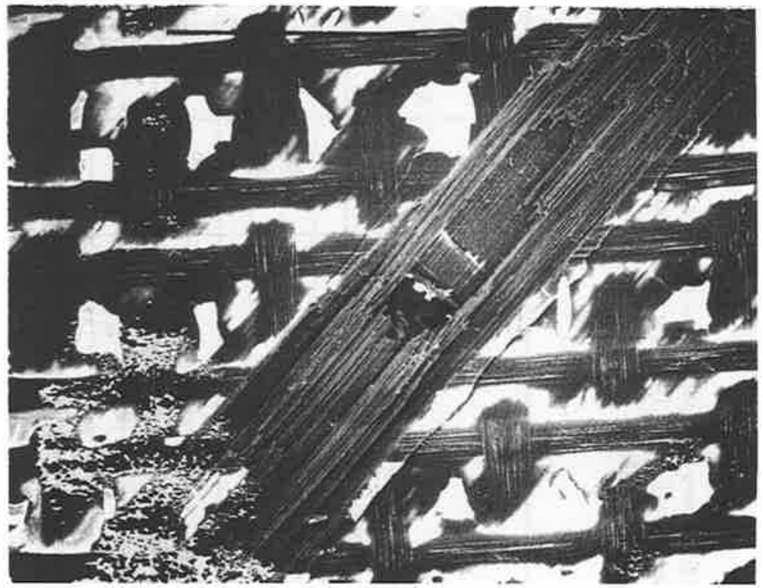

Fig. 4 View of exit face damage to composite laminate (x35)

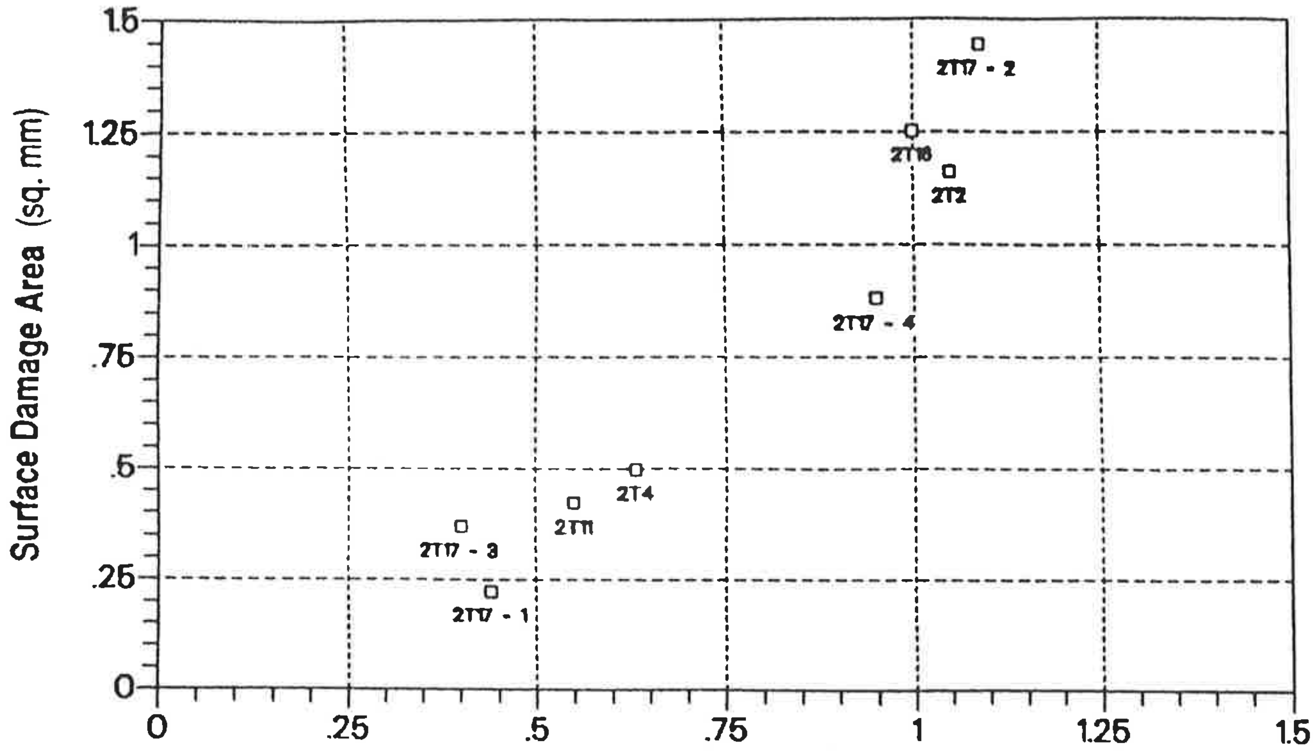

Fig. 6

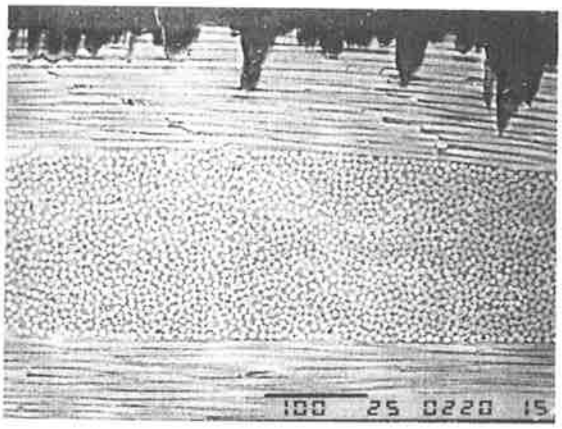

Material: P1700/T300
ROW 9 (8° off RAM)

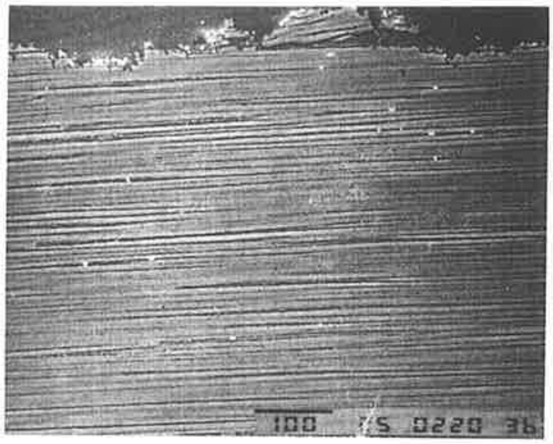

Material: 934/T300
ROW 10 (22° off RAM)

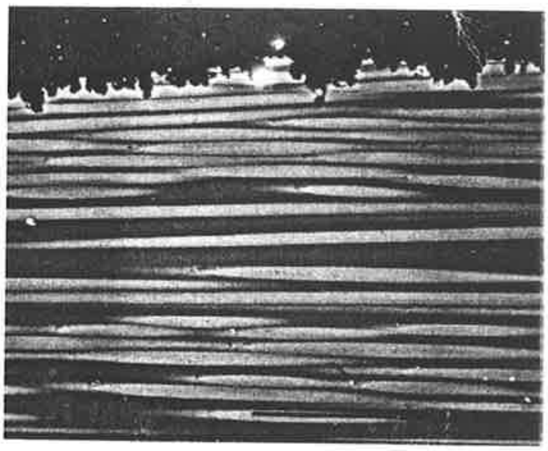

Material: PMR15/C600
ROW 7 (68° off RAM)

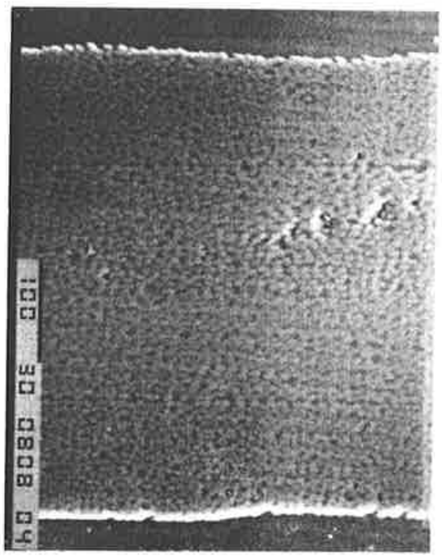

Material: 934/T300
ROW 12 (82° off RAM)

Fig. 7

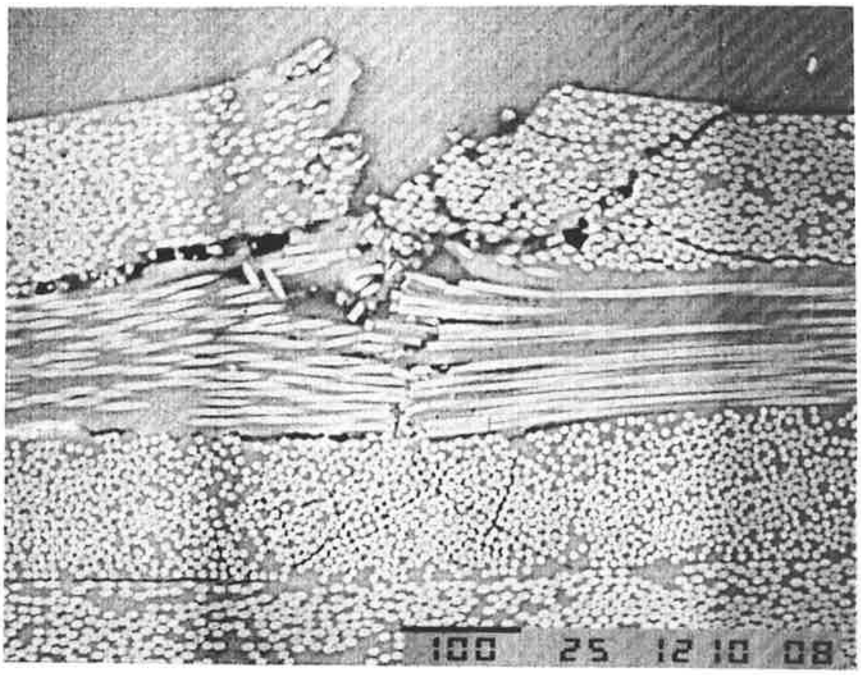

Fig. 8 Close up of Upper Half of Laminate Showing Damage in Underlying Plies

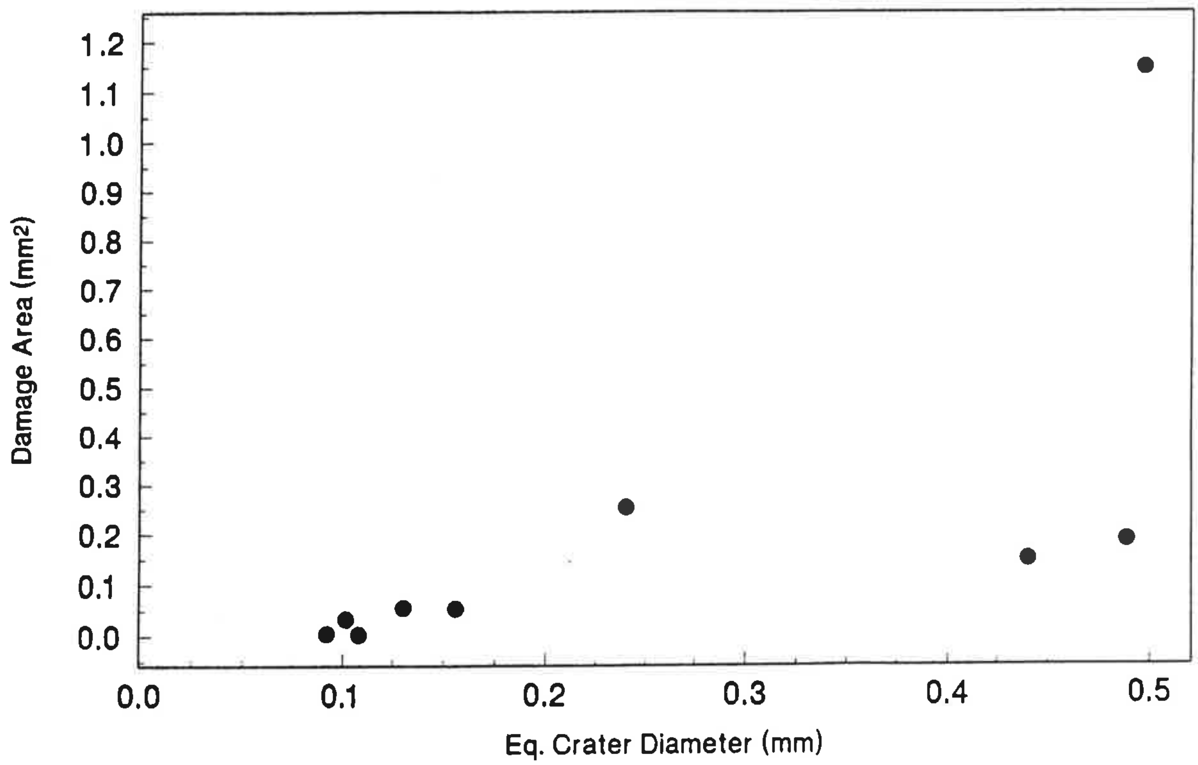

Fig. 9 Hypervelocity Impact Simulation #1
Damage Area vs Equivalent Crater Diameter